FeSb$_2$: Prototype of huge electron-diffusion thermoelectricity

Peijie Sun,[1] Niels Oeschler,[1] Simon Johnsen,[2] Bo Brummerstedt Iversen,[2] and Frank Steglich[1]

[1]*Max Planck Institute for Chemical Physics of Solids, D-01187 Dresden, Germany*
[2]*Department of Chemistry, University of Aarhus, DK-8000 Aarhus C, Denmark*
(Received 3 April 2009; published 29 April 2009)

Huge negative values of both the thermopower, $S = -10$ mV/K at 10 K, and the Nernst coefficient, $\nu = -550$ μV/K T at 7.5 K, are observed for FeSb$_2$, a narrow-gap semiconductor showing strong indications of correlation effects. A semiquantitative interpretation based on electron diffusion is presented, which suggests that the dominant term in $S(T)$, although electronic in origin, is enhanced by a factor larger than 10. This is ascribed to the presence of electron-electron correlations in FeSb$_2$ and excludes phonon drag as the dominating mechanism for the large thermopower. The correlation-enhanced thermoelectricity is of great interest for theoretical exploration as well as potential application in cooling devices at cryogenic temperatures.

PACS number(s): 72.20.Pa, 71.27.+a, 71.28.+d

Recent work shows that FeSb$_2$ shares considerable analogies with FeSi,[1–6] the unique d-electron-based correlated semiconductor. The correlated electrons in FeSb$_2$ manifest themselves in its thermodynamic properties: for instance, the magnetic susceptibility reveals thermally activated enhanced paramagnetism above 50 K (Fig. 1) and the optical spectral weight suppressed due to the gap opening is recovered only above 1 eV, a rather high energy relative to that of the gap.[5] Remarkably, Bentien *et al.*[7] found a colossal thermopower $S \approx -45$ mV/K and a huge thermoelectric power factor PF$=S^2/\rho \approx 2300$ μW/K^2 cm at around 10 K in FeSb$_2$. S is the largest ever observed in d-electron systems and the PF exceeds the values in state of the art Bi$_2$Te$_3$-based thermoelectrics by nearly 2 orders of magnitude. The origin of the huge thermoelectricity is of great interest. A comparison of FeSb$_2$ to its isostructural homolog RuSb$_2$ suggests the existence of an extra contribution from correlated electrons to the former: the magnetic susceptibility of RuSb$_2$ reveals an almost T-independent diamagnetic behavior which is strikingly different from FeSb$_2$ (Fig. 1) and indicative of the lack of significant correlation effects. Accordingly, in spite of their very similar values of charge-carrier concentration and thermal conductivity,[8] the two semiconductors exhibit values of the PF that differ by as much as 2 orders of magnitude at low T (cf. inset of Fig. 1).

In general, the thermopower arises from two distinct processes, i.e., diffusive motion of charge carriers and phonon-drag effect. We will provide evidence that the huge low-T thermopower of FeSb$_2$ does originate in the former, which provides the basis for possible thermoelectric application. The factor of 10 smaller thermopower in RuSb$_2$ (Ref. 8) is most likely dominated by the phonon drag and serves as an estimation for the phonon-drag contribution in FeSb$_2$. The prevalent theory based on a parabolic band, in the absence of correlation effects, can, at least *qualitatively*, describe the observed $S(T)$ behavior. A *semiquantitative* comparison, however, requires an additional factor larger than 10, which is very likely due to the electron-electron correlations, in particular the nonparabolicity of the correlated bands at the gap edges.

The sample (dimensions: $4.5 \times 2.0 \times 0.4$ mm^3) was cut from a single crystal prepared by chemical vapor transport

and oriented by Laue diffraction. Powder x-ray spectra confirmed its proper marcasite structure. Thermopower S, Nernst coefficient ν, and thermal conductivity κ were simultaneously measured in a homemade cryostat with a Au(Fe0.07%)-Chromel thermocouple to detect the temperature gradient. Particularly, $\nu = N/B = \frac{E_y}{B_z|\Delta T|} \frac{L}{W}$ was obtained by detecting electric potential E_y with $-\Delta T$ applied along $\vec{x}$ and magnetic field B along $\vec{z}$, L is the length, and W is the width of the sample. To eliminate any longitudinal voltage caused by contact misalignment, the Nernst measurements were repeated under opposite fields to get the average value. The Hall coefficient was measured by isothermally sweeping the magnetic field and the electrical resistivity by a conventional four-contact method. The electrical or heat current was applied along the c axis in all measurements, while B along the a axis in the measurements of ν.

The two energy gaps estimated from the resistivity (Fig. 2), $E_{g1} = 52(\pm 8)$ K and $E_{g2} = 350(\pm 30)$ K, are in good agreement with the observations made on previous FeSb$_2$ prepared by self-flux method.[7] The Hall coefficient, R_H, is negative up to at least 200 K indicating dominant electron
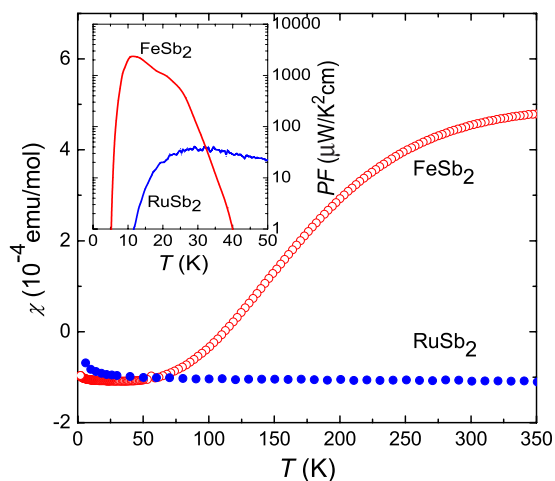

FIG. 1. (Color online) Magnetic susceptibility $\chi(T)$ and the thermoelectric power factor PF(T) (inset) of FeSb$_2$ and RuSb$_2$ (Refs. 7 and 8).
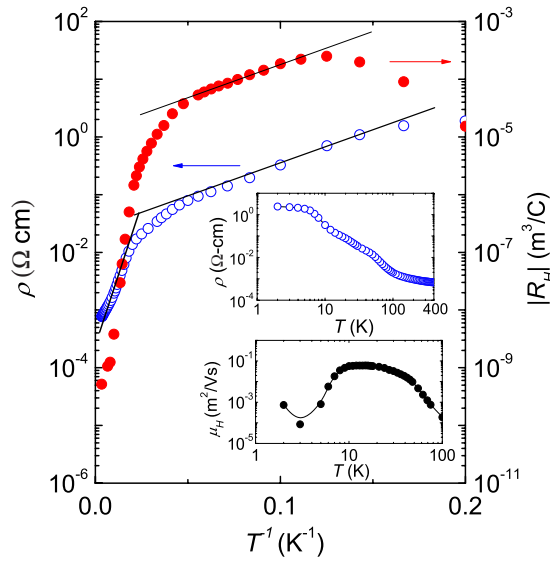
FIG. 2. (Color online) Arrhenius plots of ρ and $|R_H|$ for FeSb$_2$. Fitting $\rho(T)$ in the linear regimes, 7–20 and 50–200 K, to the thermal activation function $\rho = \rho_0 \exp(E_g/2T)$, one obtains two energy gaps $E_{g1} = 52(\pm 8)$ K and $E_{g2} = 350(\pm 30)$ K, respectively. In the range of 10–20 K, $|R_H(T)|$ is also thermally activated, showing a similarly small gap of 54 K. Upper inset displays ρ vs log T. Lower inset shows T-dependent Hall mobility μ_H.

transport. In the range of 10–20 K, a similar activation gap of 54 K of $R_H(T)$ to E_{g1} supports our notion that the evolution of ρ at low T is dominated by the thermal activation of charge carriers. Within the one-band model, the charge-carrier concentration $n = 1/e|R_H|$ varies by as much as 5 orders of magnitude from 3.5×10^{22} m^{-3} at 10 K to 2.0×10^{27} m^{-3} at 100 K, characteristic of the narrow-gap and narrow-band features common to correlated semiconductors. The high Hall mobility μ_H ($= |R_H|/\rho$) below 30 K (lower inset of Fig. 2) gives rise to the relatively high electrical conductivity and thus contributes to the large PF. A two-band analysis by Hu *et al.*[9] yields not only an even higher μ_H but also an additional subband with much (more than 6 orders of magnitude) smaller mobility. The remarkably different carrier mobilities in the two bands justify the choice of the one-band description when analyzing the transport properties. An almost flat $\rho(T)$, along with a drop in $R_H(T)$, is observed below $T \approx 7$ K (insets of Fig. 2). While such behavior is usually ascribed to the onset of *extrinsic* impurity-band conduction, for correlated semiconductors, this may be caused by the formation of a pseudogap in a narrow *intrinsic* band as observed, e.g., for CeNiSn.[10]

Both the thermopower $S(T)$ and the Nernst coefficient $\nu(T)$ are negative in the whole T range measured, 1.6–70 K (Fig. 3). $|S(T)|$ exhibits a huge peak value exceeding 10 mV/K near 10 K with the corresponding maximum PF amounting to 650 μW/cm K^2. Given the different sample preparation and measurement techniques, our results confirm the extraordinarily enhanced S and PF previously reported.[7] For a classical semiconductor, Goldsmid and Sharp[11] proposed a simple formula to relate a given energy gap to the thermopower maximum $S_{\max}$, $S_{\max} = E_g/2eT_{\max}$, where $T_{\max}$ marks the position of the peak. Using the experimental val-
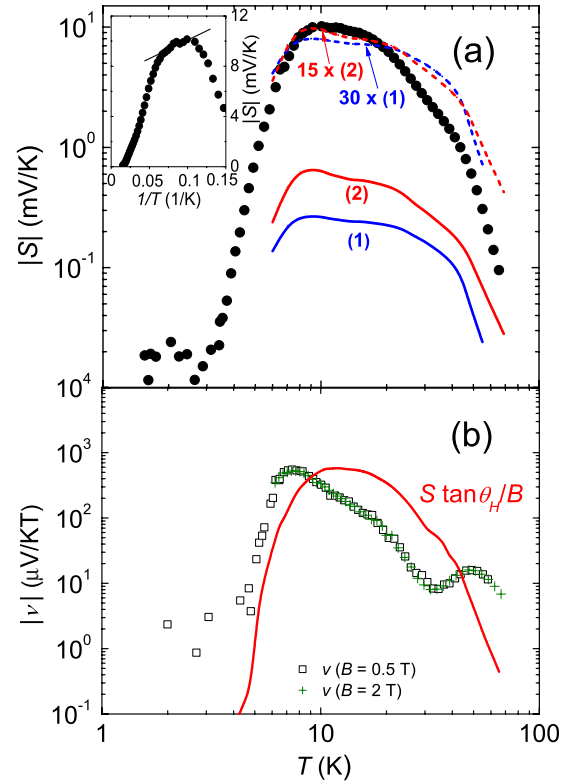

FIG. 3. (Color online) Absolute values of (a) the thermopower $S(T)$ and (b) the Nernst coefficient $\nu(T)$. $|S(T)|$ is qualitatively described by curves (1) and (2) based on Eqs. (1) and (2) with $m^* = m_0$ (see text). By applying a factor of 30 (respectively, 15) to these curves, the measured data are well described. Inset shows a plot of $|S|$ vs $1/T$. $|\nu(T)|$ is measured in $B = 0.5$ and 2 T, and is compared to the calculated curve $S \tan \theta_H/B$ (see text).

ues, $T_{\max} = 10$ K and $E_g = E_{g2} \approx 30$ meV (the larger one of the two gaps), we can estimate the classical upper limit for FeSb$_2$: $S_{\max} = 1.5$ mV/K, a value much smaller than the experimentally observed one.

As seen in Fig. 3(b), the $|\nu(T)|$ curves for $B = 0.5$ and 2 T lie on top of each other. They exhibit two maxima at 7.5 and 50 K. The first peak occurs somewhat below $T_{\max}$ of $S(T)$ and amounts to a large value of 550 μV/K T. The second one of 20 μV/K T at 50 K coincides with the pronounced drop in $|S(T)|$. Straightforwardly, we relate the double-peak structure of $|\nu(T)|$ to the double gaps obtained from $\rho(T)$. It is however worth noting that while both S and ν are strongly enhanced in the very same T range their temperature profiles look quite different. This indicates that the phonon-drag effect can only be of minor importance for the unique thermoelectric properties. This mechanism would enhance both $S(T)$ and $\nu(T)$ in a similar way, as observed, e.g., in Bi.[12]

In the following, our observations are discussed in the light of available theoretical approaches. The thermally activated carrier concentration and the T-independent Hall mobility in 10–20 K suggest a thermally activated thermopower,[13] $S(T) = \frac{k_B}{e} \frac{E_g}{2k_BT} + C$, where C is a material-dependent parameter. Such a linear dependence of $S(T)$ on $1/T$ is indeed observed in the aforementioned T range [inset of Fig. 3(a)]. However, the fit yields $E_g \approx 840$ K, a value

larger by a factor of 16 than E_{g1} obtained from $R_H(T)$ and $\rho(T)$ in the same T window.

Furthermore, the experimental $S(T)$ curve can be qualitatively described within a full decade in T (7–70 K) by electron diffusion in either a nondegenerate system,[14]

$$S(T) = \pm \frac{k_B}{e}\left[\eta - \left(r + \frac{5}{2}\right)\right], \qquad (1)$$

or, alternatively, by assuming a single-degenerate parabolic band,[15]

$$S(T) = \pm \frac{\pi^2}{3}\frac{k_B}{e}\frac{k_B T}{\epsilon_F}\left(r + \frac{3}{2}\right). \qquad (2)$$

The Fermi energy ϵ_F in Eq. (2) (degenerate regime) is estimated within the free-electron approximation, $\epsilon_F = h^2/2m^*(3n/8\pi)^{2/3}$, by using $m^* = m_0$, the free-electron mass, and n estimated from the Hall-effect results. The carrier scattering parameter r usually varies between $-\frac{1}{2}$ and $\frac{3}{2}$. Here, it is assumed to be $-\frac{1}{2}$ which, however, is not critical to the results. The reduced Fermi energy η in Eq. (1) (nondegenerate regime) is related to n and m^* via $n = 2(\frac{2\pi m^* k_B T}{h^2})^{3/2}\exp \eta$.[14] η is a convenient measure of the carrier degeneracy. Choosing $m^* = m_0$, η is found to vary between -1.5 and $+3$ in the temperature range measured. These values suggest that the present system lies in between the two regimes[16] and prove the necessity to try both approaches.

Curves (1) and (2) displayed in Fig. 3(a) are based on Eqs. (1) and (2), respectively. Apart from the magnitude, both curves provide a good description of the measured $S(T)$. In particular, they reproduce the distinct features at around 10, 20, and 50 K. This supports our interpretation that the enhanced thermopower is dominated by electron diffusion. A predominating phonon-drag effect would completely smear out the characteristic T dependence of S and furnish a single peak at $T \approx 15$ K, where the lattice thermal conductivity assumes its maximum (cf. Fig. 4 and discussion below). Also for FeSi the large thermopower has been attributed to the diffusion part of the thermopower rather than to the phonon-drag effect.[17] The close resemblance of the two theoretical curves corroborates our argument that the carrier system is on the borderline between being degenerate and nondegenerate, i.e., the measurement temperatures are in the proximity of the effective Fermi temperature, T_F^*.

To describe the observed $S(T)$ behavior *semiquantitatively*, enhancement factors are required. Curve (1) multiplied by a factor of 30 reproduces the measured data rather well, whereas a factor of 15 is needed for curve (2). These factors are in fair agreement with the one (i.e., 16) found from the thermally activated $S(T)$. Thus, given an extra factor of this size applying to all the equations in addition to the fundamental ratio k_B/e, the thermoelectric properties of FeSb$_2$ can be satisfactorily described. Similar phenomena were found in low-dimensional systems, e.g., the two-dimensional electron gas in SrTiO$_3$ causes a fivefold enhanced thermopower, relative to the classical expression of Eq. (1) which is indeed valid in the case of bulk SrTiO$_3$ (Ref. 18). Alternatively, in the degenerate regime, an enhanced ef-
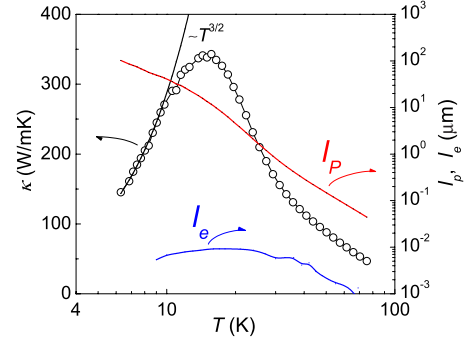

FIG. 4. (Color online) Thermal conductivity κ and mean-free path of phonons, l_p, and electrons, l_e. l_p was estimated by the kinetic formula $\kappa_L = \frac{1}{3}C_L v_s l_p$ with sound velocity $v_s = 3116$ ms^{-1} (Ref. 7), where κ_L is the lattice contribution to thermal conductivity, practically identical to κ as measured (see text), and C_L is the lattice contribution to the specific heat (Ref. 2). l_e was determined within the Drude theory, $l_e = m^* v_e / \rho n e^2$, with $v_e = \sqrt{3k_B T/m^*}$ being the thermal velocity of the conduction electrons and $m^* = m_0$.

fective charge-carrier mass m^* as inferred from susceptibility (Fig. 1) and specific heat[2] may also effectively enhance $|S|$ while maintaining its T dependence through Eq. (2). However, the case of FeSb$_2$ does not appear to be that simple. While the enhancement of m^* in FeSb$_2$, i.e., the reduction in T_F^*, would cause the carriers to be more nondegenerate, a large m^* in Eq. (1) is by far not sufficient to explain the large $S(T)$ peak. Clearly, an adequate theoretical treatment of strongly correlated semiconductors at $T \approx T_F^*$ is badly needed. Lacking such a theory, we have attempted to take the strong electronic correlations in FeSb$_2$ into account by inserting an extra factor of order 10–30 into the "classical" equations mentioned above. This approach is corroborated by 1 order of magnitude smaller (probably phonon-drag dominated) thermopower as observed in the noncorrelated reference RuSb$_2$ (inset of Fig. 1 and Ref. 8). It is quite surprising that a constant factor added to the above classical equations is apt to take into account the strong electronic correlations and the nonparabolicity induced by them at the gap edges in FeSb$_2$.

The importance of electron-electron correlations contributing to the thermoelectricity of FeSb$_2$ is further supported by the results of $\nu(T)$. Generally, there are two contributions to the electron-diffusion part of the Nernst coefficient.[19] The first one arises from the energy dependence of the carrier scattering time τ at the Fermi level. Second, there is the so-called ambipolar effect which occurs in intrinsic and compensated semiconductors and could be very large. The former effect, which is dominating in simple metals or degenerate semiconductors, is usually rather small: the upper limit of N ($=\nu B$) amounts to 40 μV/K as predicted by the classical theory.[20] Since there are no compensation features observed in R_H in the T range where $|\nu(T)|$ has a peak, the largely enhanced $|\nu|$ signals in FeSb$_2$ are most likely *not* due to the ambipolar effect. This means that the contribution due to the energy-dependent τ must be the primary reason for the observed Nernst signal, although this is largely exceeding the classical upper limit.

By introducing the Hall angle $\tan\theta_H$ ($=\mu_H B$), the contri-

bution from the energy-dependent τ can be related to the thermopower through $\nu = S \tan \theta_H / B$, which sets the upper limit of the Nernst coefficient in the absence of the ambipolar effect.[21] Figure 3(b) demonstrates that $S \tan \theta_H / B$ does indeed yield a good order-of-magnitude description of the observed $|\nu(T)|$, which lends further support to the argument that the Nernst signal in FeSb$_2$ is primarily dictated by the energy dependence of τ: an enhanced $\partial \tau / \partial \epsilon$, accompanying the onset of the two gaps is the likely source of the double-peak structure of $|\nu(T)|$. In combination with the correlation-enhanced diffusion thermopower this brings about the large Nernst signals with the peculiar structure.

Figure 4 shows the T dependence of both the thermal conductivity κ and the mean-free path l of phonons and electrons, respectively. The electronic contribution $\kappa_e(T)$ estimated via the Wiedemann-Franz law is negligibly small (less than 0.1% for $T < 75$ K). A large $\kappa(T)$ maximum of 350 W/mK is observed at 15 K, followed by a $T^{3/2}$ dependence below 10 K. The phonon mean-free path $l_p(T)$ is found to increase monotonically upon cooling, showing a weak change in slope at 15 K where $\kappa(T)$ assumes its peak. No anomaly can be resolved at 10 K, the position of $S_{\max}$. At this temperature, $l_p \approx 40$ μm is still 1 order of magnitude smaller than the sample thickness. On the other hand, the electron mean-free path l_e is less than 10 nm at all temperatures, more than 2 orders of magnitude shorter than l_p. Vis-à-vis, this extremely large difference in mean-free paths, it appears fea-

sible to minimize κ by, e.g., introducing spatially extended scatterers to the propagating phonons while almost maintaining the huge PF. This would enhance the thermoelectric dimensionless figure of merit $ZT = T(PF/\kappa)$ at low temperatures substantially.

In conclusion, we have observed largely enhanced $|S(T)|$ and $|\nu(T)|$ values in FeSb$_2$. The dominance of electron diffusion rather than phonon-drag effect in the enhanced thermoelectricity is identified by: (i) the factor-of-10 enhanced thermopower of correlated FeSb$_2$ relative to the noncorrelated reference RuSb$_2$; (ii) the huge thermopower of FeSb$_2$ which follows the classical features of diffusive electrons, although an enhancement factor presumably caused by electron correlations is necessary for an quantitative description; and (iii) the completely different temperature profiles of $|S(T)|$ and $|\nu(T)|$ differing from what is expected for a phonon-drag dominated system and the double-peak structure of $|\nu(T)|$ being readily explained by enhanced values of $\partial \tau / \partial \epsilon$ due to the opening of the two energy gaps. Our results, which clearly indicate the importance of electron correlations in thermoelectricity, are of considerable interest for both thermoelectric application at cryogenic temperatures and theoretical exploration.

[1] D. Mandrus, J. L. Sarrao, A. Migliori, J. D. Thompson, and Z. Fisk, Phys. Rev. B **51**, 4763 (1995).

[2] A. Bentien, G. K. H. Madsen, S. Johnsen, and B. B. Iversen, Phys. Rev. B **74**, 205105 (2006).

[3] C. Petrovic, Y. Lee, T. Vogt, N. Dj. Lazarov, S. L. Bud'ko, and P. C. Canfield, Phys. Rev. B **72**, 045103 (2005).

[4] C. Petrovic, J. W. Kim, S. L. Bud'ko, A. I. Goldman, P. C. Canfield, W. Choe, and G. J. Miller, Phys. Rev. B **67**, 155205 (2003).

[5] A. Perucchi, L. Degiorgi, R. Hu, C. Petrovic, and V. F. Mitrović, Eur. Phys. J. B **54**, 175 (2006).

[6] A. V. Lukoyanov, V. V. Mazurenko, V. I. Anisimov, M. Sigrist, and T. M. Rice, Eur. Phys. J. B **53**, 205 (2006).

[7] A. Bentien, S. Johnsen, G. K. H. Madsen, B. B. Iversen, and F. Steglich, EPL **80**, 17008 (2007).

[8] P. Sun, N. Oeschler, S. Johnsen, B. B. Iversen, and F. Steglich, J. Phys.: Conf. Ser. **150**, 012049 (2009).

[9] R. Hu, V. F. Mitrović, and C. Petrovic, Appl. Phys. Lett. **92**, 182108 (2008).

[10] K. Izawa, T. Suzuki, T. Fujita, T. Takabatake, G. Nakamoto, H. Fujii, and K. Maezawa, Phys. Rev. B **59**, 2599 (1999).

[11] H. J. Goldsmid and J. W. Sharp, J. Electron. Mater. **28**, 869 (1999).

[12] K. Behnia, M. A. Méasson, and Y. Kopelevich, Phys. Rev. Lett. **98**, 076603 (2007); V. D. Kagan *et al.*, Phys. Solid State **46**, 1410 (2004).

[13] H. Fritzsche, Solid State Commun. **9**, 1813 (1971).

[14] G. S. Nolas, J. Sharp, and H. J. Goldsmid, *Thermoelectrics: Basic Principles and New Materials Developmemts* (Springer, Berlin, 2001).

[15] K. Behnia, D. Jaccard, and J. Flouquet, J. Phys.: Condens. Matter **16**, 5187 (2004).

[16] The nondegenerate (degenerate) approximation applies when $\eta \ll 0$ ($\eta \gg 0$).

[17] T. Jarlborg, Phys. Rev. B **51**, 11106 (1995).

[18] H. Ohta, S. Kimu, Y. Mune, T. Mizoguchi, K. Nomura, S. Ohta, T. Nomura, Y. Nakanishi, Y. Ikuhara, M. Hirano, H. Hosono, and K. Koumoto, Nature Mater. **6**, 129 (2007).

[19] R. T. Delves, Rep. Prog. Phys. **28**, 249 (1965).

[20] T. C. Harman, Appl. Phys. Lett. **2**, 13 (1963).

[21] Y. Wang, Z. A. Xu, T. Kakeshita, S. Uchida, S. Ono, Y. Ando, and N. P. Ong, Phys. Rev. B **64**, 224519 (2001).